Journal of Engineering Research Innovation and Scientific Development 3 (1), (2025), 1-13 https://doi.org/10.61448/jerisd31251

Journal of Engineering Research Innovation and Scientific Development
journal homepage: www.jerisddelsu.com
Print ISSN 2971-6594 Online ISSN 2971-6608

Design and Fabrication of a Dual-Phase Cascade Refrigeration System for Efficient Cold Storage and Healthcare Services

Olarewaju Thomas Oginni

Department of Mechanical Engineering, School of Engineering Technology, Bamidele Olumilua University of Education, Science and Technology, Ikere-Ekiti (BOUESTI), Nigeria.

Corresponding Author Email: oginni.olarewaju@bouesti.edu.ng

ARTICLE HISTORY

Received: 10-01-25
Revised: 15-02-25
Accepted: 20-02-25
Published: 28-02-25

ABSTRACT

Human blood plasma storage faces challenges like cold conditions, quality surveillance, stable freezing, and reliable facilities, while clinics lack transit chilling for quick processing at collection centres. A portable vapour compression chiller (PVCC) offers a secure solution for handling heat-susceptible items, addressing international health security risks, and delivering safe medical care in underdeveloped nations. Employing a copper tube evaporator (CTE) in contrast to a blast evaporator (BE), the research examines an improved dual-stage vapour compression cascade technique (DSVCCT) that incorporates a storage compartment. A 12 kg storage capacity, 5 kVA generator provides a rapid, ultra-low temperature time-freezing temperature evaporator tested with cow blood plasma and monitored for freezer temperature decline and distribution. The system measurements are conducted to analyze the pull-down time (PDT), defrosting time (DT), power consumption (PC), coefficient of performance (COP), and overall efficiency (OE) at the different intermediate cascade temperatures. The system achieved -20°C with a pull-down time of 420 minutes, demonstrating 89.6% efficiency and 415.8 MJ and 105.6 MJ energy usage for copper tubes and blast evaporators, respectively. The refrigerating effect was recorded at 140.9 kJ/kg and 3.18 COP. The refrigerating effect was 140.9 kJ/kg and 3.18 COP. The modified refrigeration technique has been found to extend plasma refrigeration systems' shelf life by four days off-cycle, saving 4.62 MJ of energy at zero emissions and cost-effectively. The design is energy-efficient, suitable for energy-deficient economies due to its longer shelf life and portability, making it ideal for transporting and managing heat-sensitive drugs in healthcare areas with limited resources.

Keywords: Efficiency; healthcare; portability; power consumption; refrigerating technique

1. Introduction

The cascade refrigeration system is a promising low-temperature technology that utilizes an energy-efficient cycle for rapid freezing and maintaining desired storage temperatures (The machine's potential in various fields, including medicine, biology, business, agriculture, and industry, has sparked interest from academia and industry due to its numerous benefits (Rangare and Mishra, 2019).This system operates in frigid temperatures, with frozen cabinets' evaporating temperatures operating below -18°C (Oginni*et al.,* 2024). For instance, cascade refrigeration technology is utilized in blood banks to preserve biological fluids like plasma and vaccines, but heat-sensitive immunizations may be challenging due to limited ultra-low temperature cold storage (WHO, 2022).

The cascade cycle is utilized for large temperature ranges, enhancing the refrigeration cycle coefficient of performance and allowing for adequate evaporator and condenser pressures by using refrigerants with decreasing boiling points (Shukla *et al.,* 2018). Figure 1presents a cascade condenser that links the lower and higher temperature cycles together. It consists of a compressor, condenser, evaporator, heat exchanger, and throttle devices. The two single-stage refrigeration systems are connected in series to create a cascade system, with the lower system (PSS) maintaining a lower evaporating temperature and the upper system (SSS) extracting heat through a cascade condenser. Processes "a-b" compress low-pressure and low-temperature refrigerants isentropically, while operations "c-d" transfer heat to higher-temperature and pressure refrigerants. Processes "e-f" involve compressing, rejecting, and expanding. The refrigerant undergoes a throttling process of "g-h" by expanding isentropically, then moves to a cascade condenser for heat transfer between two refrigerants (Oginni*et al.*, 2023; Pan *et al*., 2020; Ustaoglu *et al.*, 2020).

In many industries and medical sectors, the time to achieve the desired temperature is paramount. Refrigerants R410A and R404A were chosen for rapid homogeneous freezing and storing fresh blood plasma (Nagraju *et al.*, 2015). In terms of refrigerating effect and discharge pressure, R410A is slightly better than that of R22, achieving low temperatures in a short time. R404A is recommended for domestic refrigeration purposes, while R410A is preferred over R22 due to its better mass flow rate (Chakravarthy and Deva-kumar, 2012; Zhou *et al.*, 2018).

Global vaccine delivery is a complex task requiring meticulous storage, handling, and transportation in temperature-controlled environments. Research reveals blood donation and healthcare centers lack mobile refrigeration facilities for plasma preparation (Mota-Babiloni *et al.*, 2020). A revolutionary design for a mobile device that optimizes processing and storage for secure delivery at all healthcare levels is required(Zhang *et al.,* 2022; Lemboye *et al.*, 2015). Plasma consists of 91% to 92% water, with the remaining 8% to 9% comprising glucose, hormones, proteins, minerals, vitamins, waste materials, clotting factors, immunoglobulins, and carbon dioxide (Alhumaidan *et al.*, 2010). It is essential for blood components to flow around the body and is primarily water absorbed by the intestines from consumed food and liquids (Upadhyay and Pangtey, 2016; Adkins *et al.*, 2022).Blood plasma preservation faces challenges in maintaining stable, low-temperature environments, monitoring plasma quality, delayed freezing periods, and temperature-sensitive storage systems in traditional medical freezers and procedures (Zhang et al., 2022).

The cascade refrigeration system ensures a consistent blood product supply in ultra-low temperature applications, but blood donation clinics lack a transit refrigeration system for immediate plasma processing. The study proposes a mobile copper tube-based system for efficient off-cycle freezing and defrosting, improving healthcare delivery in rural areas. It addresses processing delays, poor temperature control, and cold-storage issues, ensuring zero emissions.

2. Materials and Method

The machine, consisting of a compressor for a high-temperature circuit (HTC) and a low-temperature circuit (LTC), a condenser, expansion valves, and an electrical fan motor, was assembled using various methods. It was filled with the appropriate refrigerant and tested using pressure and temperature detectors to determine its performance coefficient. The main raw material required for system evaluation is cattle blood plasma (Gratten *et al.*, 2018). The thermodynamic analysis was simplified by assuming all components operate at a steady state, with negligible changes in kinetic and potential energy, minimal heat loss, and a pressure drop. The refrigerating chamber with suspended plasma is computer-aided, and a two-stage cascade refrigeration system is assembled for speedy freezing and compact unit assembly for mobility. The developed system parts and description are as shown in Table 1, while Figure 2 presents the machine components (Leonardo *et al.*, 2018; Chen *et al.*, 2019).

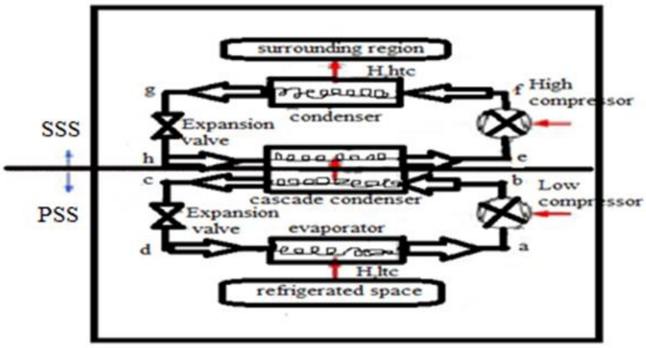

Figure 1: Dual-phase Refrigeration System (Ustaoglu et al., 2020)

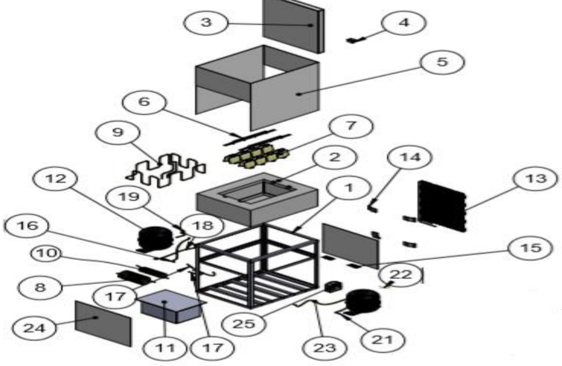

Figure 2: Machine components

Table 1: System parts and description

Item	Part Number	Description	Quantity
1	Frame	Mild steel angle iron	1
2	Insulator	Styrofoam	1
3	Cover	Stainless steel plate	1
4	Hinger	Stainless steel rod	2
5	Side plate cover	Stainless steel plate	1
6	Hangers	Mild steel	
7	Plasma bag	Paediatric bag	8
8	Cascade evaporator	8mm copper pipe	1
9	Evaporator	8mm copper pipe	1
10	Cascade container	Stainless steel plate	1
11	Cascade condenser	8mm copper pipe	1
12	Compressor	0.5 hp compressor	2
13	Condenser	8mm aluminium	1
14	Condenser holder	Mild steel plate	4
15	Capillary tube	3mm capillary tube	2
16	Tubing 1	8mm copper tube	1
17	Tubing 2	8mm copper tube	1
18	Tubing 3	8mm copper tube	1
19	Tubing 4	8mm copper tube	1
20	Tubing 5	8mm copper tube	1
21	Tubing 6	8mm copper tube	1
22	Tubing 7	8mm copper tube	1
23	Tubing 8	8mm copper tube	1
24	Front cover plate	Mild steel plate	2
25	Control	Digital control system	1

R410A and R404A are popular refrigerants for rapid homogeneous freezing and storage of blood plasma, offering superior thermodynamic properties, better discharge pressure, and mass flow rate. This making it preferred for domestic refrigeration and crucial in industries like medicine (Mondragon et al., 2018).

2.1 Cycle Analysis

2.1.1 Determination of Heat Load

The wall heat gain load measures heat transfer in a refrigerated room, influenced by temperature differential, thermal resistance, thickness, and surface area. The ambient product temperature (ATP) is 293 K, the frozen plasma temperature (FPT) is 253 K, and the change in temperature (ΔT) is 40 K. The cooling chamber insulation area is 0.37 m^2, and the heat flow rate is 0.84 kW as calculated in Equations 1 and 2 (Abdulghafor et al., 2024).

$$A_{cci} = hw + lh + wh \quad (1)$$

$$H_f = \Delta TUA \quad (2)$$

The evaporator's walls pass 912 kW of heat for three hours, crucial for cold storage, with eight (8) blood plasma bags per batch placed in the chilling chamber is estimated using Equation 3 (Prommas *et al.,* 2019).

$$H_f = H_{ew}\, t \quad (3)$$

The product load of a system is determined by dividing freezing load into three groups: chilling load above freezing, cooling load below freezing, and freezing load. The heat of 574kW is accumulated during a 2kg blood plasma cooling from 35°C to -0.59°C, which freezes at -0.59°C, as calculated using Equation 4 (Prommas *et al.,* 2019).

$$H_f = M_p C_p \Delta T_0 \quad (4)$$

The cascade system requires 2115 W of product heat load due to the additional cooling load below freezing, which requires 282 kW of heat and 1259 kW of energy as contained in Equations 5 and 6 (Tsatsaronis and Morosuk, 2018).

$$H_b = M_p C_p \Delta T_i \quad (5)$$

$$H_f = M_p L_p \quad (6)$$

The infiltration of 1.55 W air into a frigid room is influenced by temperature and size differences. 0.205 kg samples are packaged in plastic bags, resulting in a total heat gain of 4.25 W. The heat loads required for a 40% safety factor is 2.97 kW in total as determined by Equations 7 and 8 (Tsatsaronis and Morosuk, 2018).

$$H_{inf} = M_i C_a (T_0 - T_i) \quad (7)$$

$$H_{pk} = M_{pk} C_{pk} (T_0 - T_i)\, 10^3 \quad (8)$$

A 1 hp compressor is needed for 3.97 kW refrigeration, with evaporator and condenser purchased based on capacity. LTC condenser's design, 1.726 kW, and HTC condenser (Q_H), reject (H_L) 1.954 kW of heat as stated in Equations 9 to 11, respectively (Tsatsaronis and Morosuk, 2018).

$$H_r = \Delta TUA \quad (9)$$

$$H_l = m_l (h_b - h_c) \quad (10)$$

$$H_h = m_l (h_f - h_g) \quad (11)$$

2.1.2 Fabrication and System Performance Evaluation

The unit technique involved soldering, welding, and securing components like the evaporator, compressors, condenser, fan, heat exchanger, expansion valves, copper tube, and line connections. The two-stage vapour compression refrigerating system is constructed and fabricated with integrated circuit breakers for safety and digital thermocouples for efficiency computation. Figures 3 to 8 present the machine parts assembly, rear view, side view, refrigerating chamber, storage unit, and complete system assembly, respectively. The cascade freezer with a copper tube evaporator and the cascade freezer with a blast evaporator (Oginni*et al.,* 2024) for evaluation are shown in Figures 9 and 10.

Animal blood from Ekiti State veterinary farm was centrifuged at Ekiti State Teaching Hospital, Nigeria, and samples were packed into 200-ml units and frozen in the machine cooling chamber of Figures 9 and 10 having copper tubes and a blast evaporator for evaluation and comparison. Refractometer protein tests were conducted before and after freezing, evaluating system performance at no load, varying blood plasma loads, and constant load, recording the time taken to form frozen plasma.

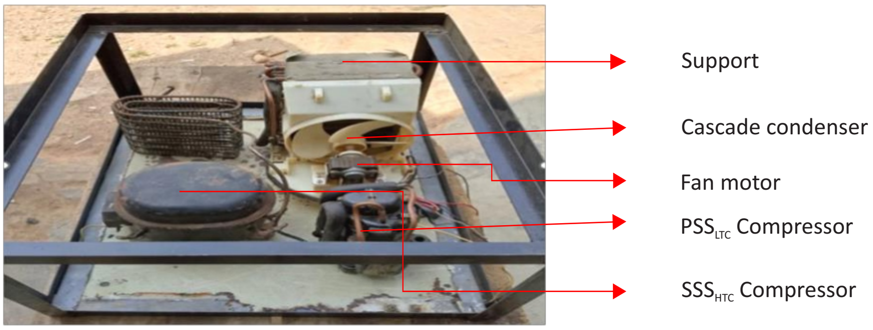

Figure 3: Machine parts assembly

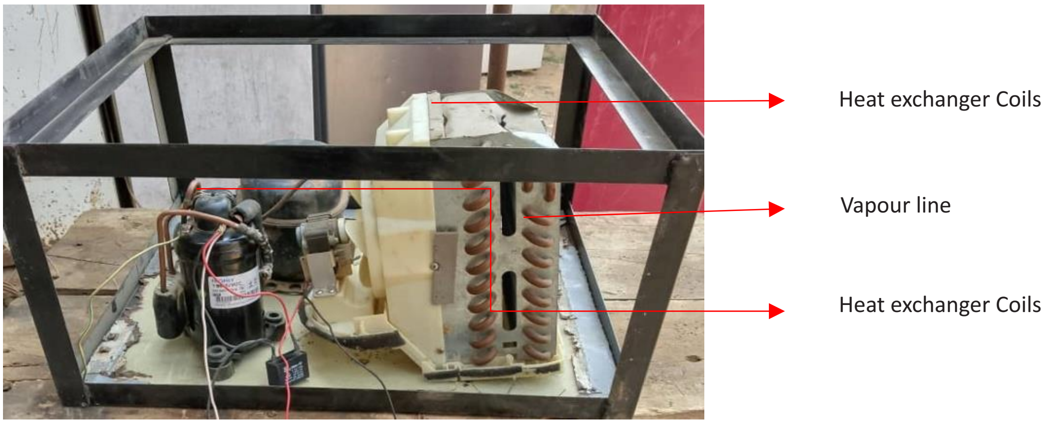

Figure 4: System rear view assembly

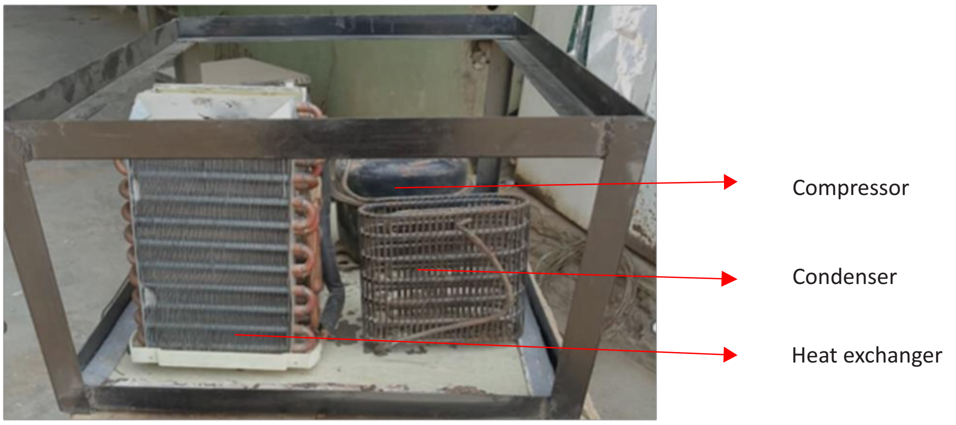

Figure 5: System Side view assembly

Figure 6: Refrigerating chamber

Figure 7: Storage unit

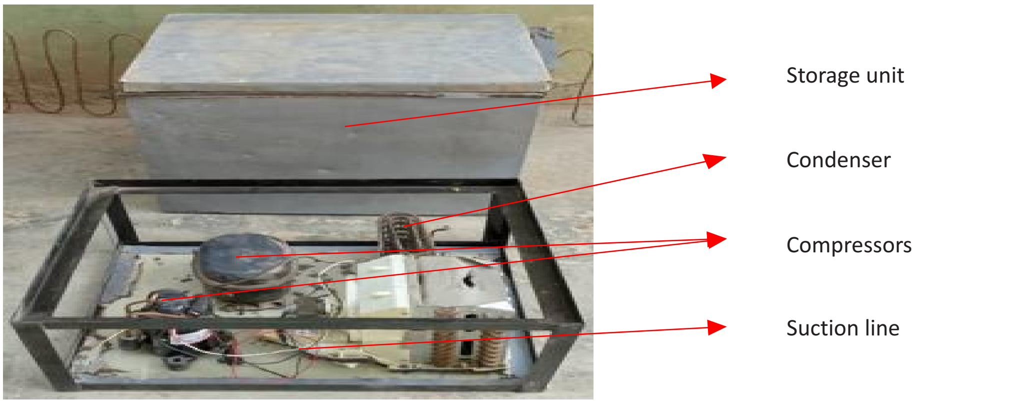

Figure 8: Complete system assembly

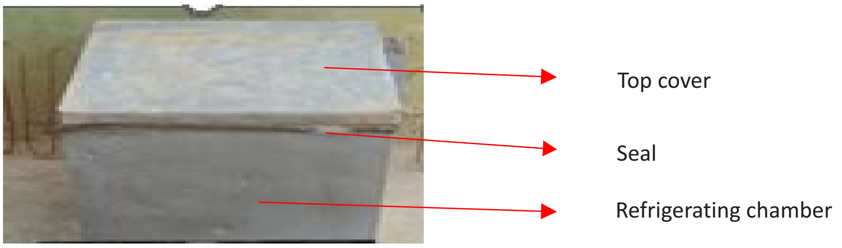

Figure 9: Cascade freezer with copper tube evaporator

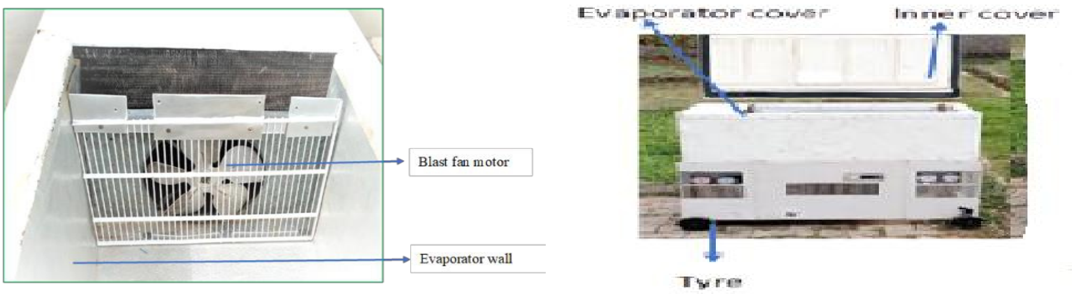

Figure 10: Cascade freezer with blast evaporator (Oginni et al., 2024).

The machine was operated under specific conditions, including varying evaporator (-20 to -4 °C), condenser (40 to 48°C), and cascade condenser temperatures (2 to 6 °C), while maintaining other parameters constant.

Table 2 presents the mathematical expressions used to obtained other results from the system performance(Wang et al., 2020; Caramello et al., 2019).

Table 2: Mathematical equations for primary (low) and secondary (high) temperature cycles

Parameters	Symbol	Primary Stage System (PSS)	Secondary Stage System (SSS)
Refrigerating effect	C_e	$C_e = h_a - h_d$	$C_{ce,h} = h_e - h_h$
Mass flow rate	$\dot{m}$	$\dot{m}_l = \frac{H_{ce}}{C_e}$	$m_h = \frac{m_l (h_b - h_c)}{(h_e - h_h)}$
Compressor pressure ratio	P_r	$P_{rl} = \frac{P_{dl}}{P_{sl}}$	$P_{rh} = \frac{P_{dh}}{P_{sh}}$
Compressor work	W_{comp}	$W_{comp,l} = (h_b - h_a)$	$W_{comp,h} = (h_f - h_e)$
Compressor power	P_{comp}	$P_{cl} = m_l - \dot{W}_{CL}$	$P_{CH} = m_H (h_6 - h_5)$
Condenser heat rejection	H_r	$H_{rl} = m_l (h_b - h_c)$	$H_{comp,h} = m_l (h_f - h_g)$
Coefficient of Performance	COP_c	$COP_l = \frac{C_e}{W_{comp,l}}$	$COP_h = \frac{C_e}{W_{comp,h}}$
Reversed Cycle COP	$COP_{ideal,l}$	$COP_{ideal,l} = \frac{t_{erl}}{t_{cr,l} - t_{e,l}}$	$COP_{ideal,h} = \frac{h}{t_{c,h} - t_{e,h}}$
System Efficiency	n_l	$n_r = \frac{COP_l}{COP_{ideal,l}}$	$n_h = \frac{COP_{a,h}}{COP_{ideal,h}}$
Cascade System COP	COP_{cas}	$COP_{cas} = \frac{COP_{a,h}}{W_{l,c} + W_{h,c}}$	
System Isentropic efficiency	I_{cas}	$I_{cas} = \frac{100W_{rev}}{W_a}$	
System's relative effectiveness	RE_{cas}	$RE_{cas} = \frac{COP_l}{COP_{ideal,l}}$	

3. Results and Discussion

3.1 Variation of Evaporator Temperature and System Pull-Down Time at No-Load

Figure 12 demonstrates temperature variations in an evaporator under no load, showing that blast and copper tube evaporators take 73 and 180 minutes to change air temperature from 35 °C to -20 °C. The duration of cooling chamber confined air experiences a cooling effect more as it takes longer (Wang *et al.*, 2020).The blast evaporator exhibits a faster cooling rate compared to the copper tube evaporator.

3.2 Variation of Evaporator Temperature with Time at Varying Load

Figure 13 shows performance assessment tests and experimental adjustments for a copper tube evaporator, comparing plasma mass proportion with frozen creation period. The freezing states of 0.512 kg, 1.024 kg, and 2.048 kg of fresh plasma masses increased gradually over time increments of 180, 250, and 420 minutes, respectively. Time significantly impacts the mass required for a new plasma to transition into its frozen stat

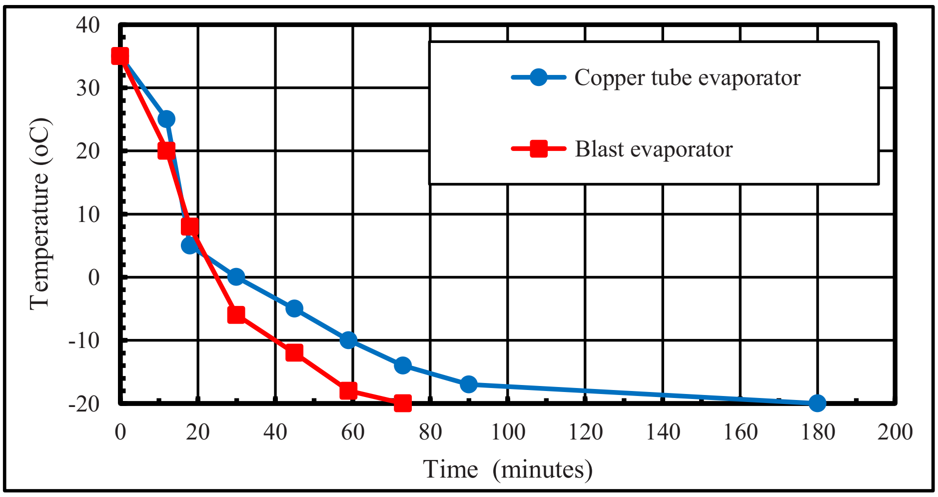

Figure 12: System pull-down time at no-load

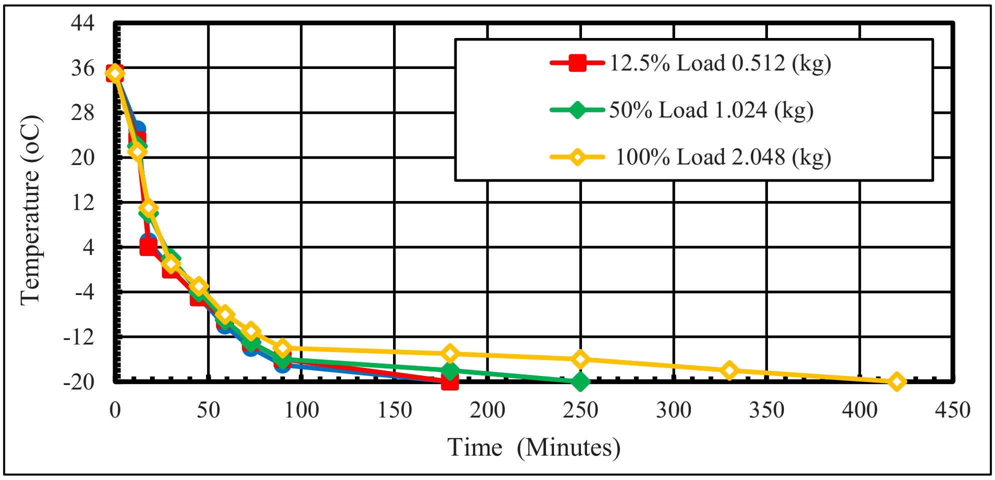

Figure 13: Cooling load temperature-time

3.3 Impact of in Evaporator, Condenser and Cascade Condenser Temperatures on Other Parameters

Table 3 outlines the impact of evaporator temperature variations from -20 °C to -4 °C on system operation at fixed and cascade condenser temperatures, citing experimental results on suction and discharge temperature. The influence of temperature changes on various evaporator variables, such as mass flow rates, coefficient of performance, and efficiencies in both cycles, was revealed. Tables 4 and 5 illustrate the effects of temperature changes in condensate and cascade condensers at 40 to 48°C elevations and 6 to 2°C, while maintaining all other parameters unchanged. The results of the impact changes in condenser temperatures and cascading response, as well as the coefficient of performance, chilling effect, and efficiencies, were presented.

Table 3: Effect of change in evaporator temperature on other parameters

T_{el}	T_{cc}	T_{ch}	COP_l	n_{pss}	COP_s	n_{sss}	$\frac{m_i}{m_h}$	R_e	COP_{cas}	n_{isent}
-20	6	40	3.62	73.6	7.14	67.5	1.64	140.9	3.18	42.0
-16	6	40	3.96	66.2	7.82	69.2	1.68	144.0	3.15	42.3
-12	6	40	4.10	58.8	8.3	77.5	1.75	146.3	3.24	43.4
-8	6	40	4.23	52.6	8.6	86.4	1.76	148.4	3.27	43.7
-4	6	40	4.30	48.8	8.9	89.6	1.69	150.6	3.36	44.5

Table 4: Effect of change in condenser temperature on other parameters

T_{el}	T_{cc}	T_{ch}	COP_l	n_{pss}	COP_s	n_{sss}	$\frac{m_i}{m_h}$	R_e	COP_{cas}	n_{isent}
-20	6	40	3.62	73.6	7.14	67.5	1.64	140.9	3.18	42.0
-20	6	42	3.46	73.0	7.02	67.6	1.68	140.0	3.00	41.6
-20	6	44	3.29	72.9	6.96	67.7	1.70	139.6	2.90	41.2
-20	6	46	3.04	72.8	6.82	67.8	1.72	139.4	2.78	40.4
-20	6	48	2.98	72.6	6.74	67.9	1.74	139.2	2.54	40.0

Table 5: Effect of variation in temperature in cascade condenser on other parameters

T_{el}	T_{cc}	T_{ch}	COP_l	n_{pss}	COP_s	n_{sss}	$\frac{m_i}{m_h}$	R_e	COP_{cas}	n_{isent}
-20	6	40	3.62	73.6	7.14	67.5	1.64	140.9	3.18	42.0
-20	5	40	3.66	73.7	7.13	66.7	1.58	141.5	3.19	41.2

-20	4	40	3.70	73.8	7.10	65.3	1.51	142.6	3.22	41.0
-20	3	40	3.74	73.9	7.12	64.8	1.48	143.8	3.39	40.4
-20	2	40	3.78	74.0	7.08	63.4	1.43	145.3	3.48	39.1

3.4 System Refrigerating Effect and Isentropic efficiency

Figure 14 shows that the refrigerating effect decreases with a higher cascade condenser temperature from 2 to 6.1 °C., while the isentropic efficacy increases from 40.13 to 41.79% with a temperature differential of 1 °C, resulting in a decrease from 140.9 to 145.3 kJ/kg. The graph indicates that the system's productivity increases with an increase in the cascade condenser temperature.

3.5 Relation between Evaporator temperature, Refrigerating Effect and COP

Figure 15 shows that the system coefficient of performance (COP) increases (3.18 to 3.36) with evaporator temperature (-20 to -4 °C), resulting in an improvement in refrigerating capacity power, as the overall COP improves with rising vaporization temperatures. The COP decreases from 3.0 to 2.54 with increased condenser temperature (40 to 48 °C), indicating a left-to-right sliding slope, indicating that higher condensing temperatures increase productivity.

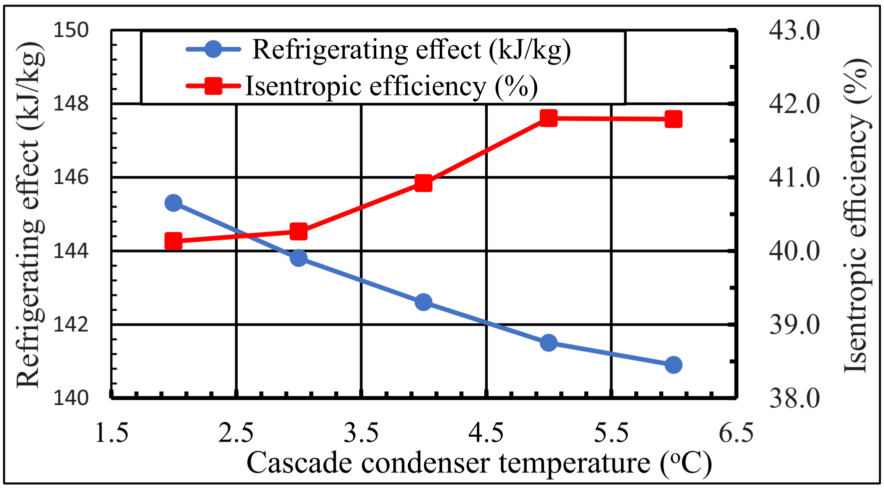

Figure 14: Refrigeraating effect against Isentropic efficiency

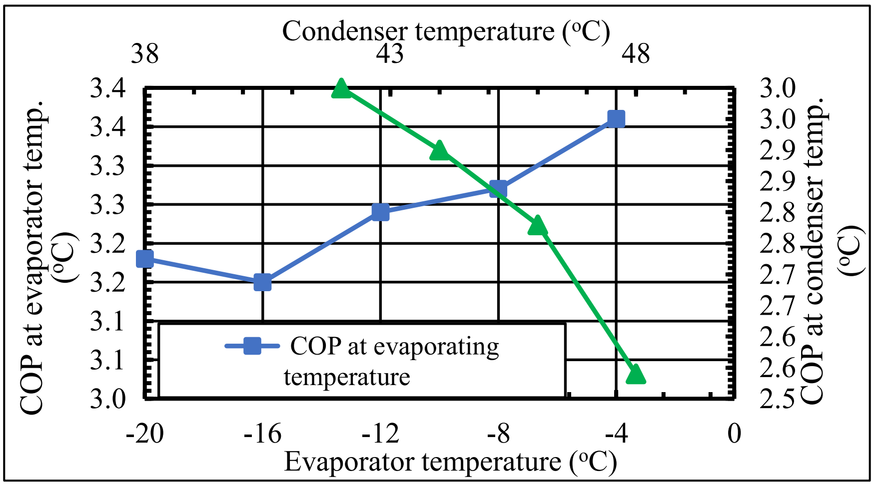

Figure 15: Evaporator temperature against refrigerating effect

3.6 Temperature Variation and Frosting and De-Frosting Time

Figure 16 displays samples of fresh frozen plasma at -20°C stored for stable temperature and defrosting period monitoring via off-cycle. Figure 17 illustrates the freezing rate of fresh plasma and its impact on temperature variation. It takes 420 minutes to freeze plasma from 35 °C to -20 °C using a copper tube evaporator. The system maintains plasma nutritional value for 76 hours at -20 °C, retaining its fresh state. The machine is suitable for plasma management, quick freezing storage, and distribution of heat-sensitive medications and vaccines, offering energy efficiency for commercial use in both developed and developing economies.

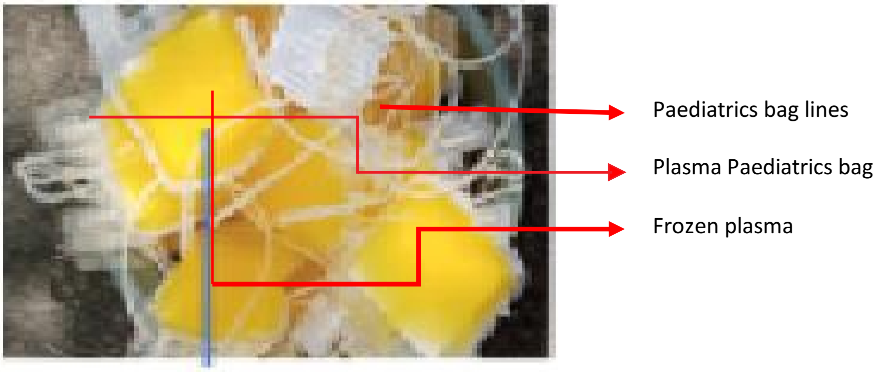

Figure 16: Sample of frozen plasma at -20 °C (Oginni *et al.*, 2024)

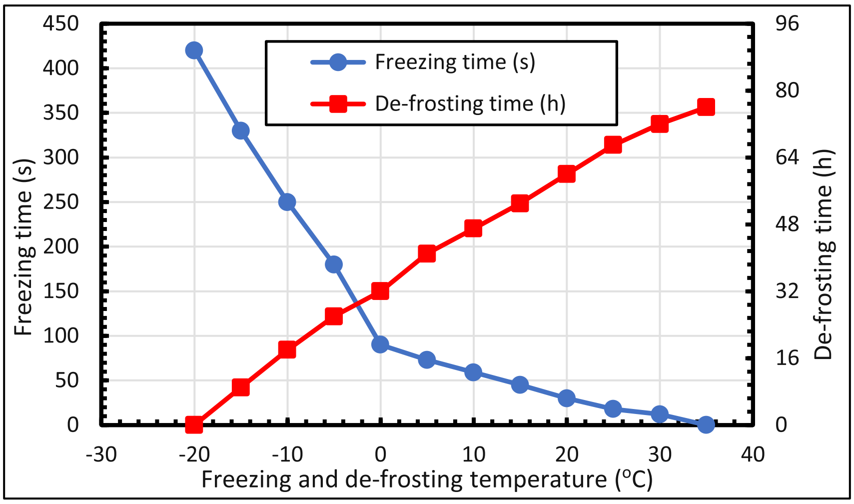

Figure 17: Frosting and De-frosting time against temperature

3.7 Comparative Analysis of Copper Tube and Blast Evaporator Freezers
Table 5 compares the energy consumption of copper coil evaporators and blast evaporator refrigerators, revealing that blast evaporator freezers are more energy-efficient and cost-effective for freezing, while copper tube evaporators show increased energy conservation off-cycle.

Table 5 :Comparative analysis of copper tube and blast evaporator freezers

Product Name	Copper tube Evaporator Machine	Blast Evaporator Machine
Hours used	6	2
Max temp.	-20°C	-20 °C
Running time (minutes)	420	80
Power consumed per day (kwh)	4620	880
Power consumed per year (MJ)	415.8	105.6
Total Energy Cost per year (Naira)	1,074,150	272,800
Heat Retention	Better	Good
Energy-saving at off-cycle	Better	Good
Cost effectiveness	Good	Better
Energy saving on-cycle	Good	Better
Frosting time	Low	High
Defrosting time	High	Low
Ice builds up	Big	Small
Door services at storage	Favored	Not-favored
Limitation of freezing temperature	Built-up ice and refrigerants	Refrigerants

3.8 Comparison of Protein Retention by Blast and Copper Tube Evaporators

As presented, Figure 18 analyzed plasma protein concentration and quality indicators before and after freezing in a temperature-controlled storage system, comparing the efficiency of cooper tubes and blast-evaporator freezers in preserving frozen plasma concentrations off-cycle. Both systems maintained raw plasma concentration for two days, except for the blast evaporator's drop after a 50-hour power outage. The plasma machine's design is cost-effective and efficient for preserving frozen plasma and transporting heat-sensitive medical goods, maintaining protein characteristics for transfusion (Prommas *et al.*, 2019; Tsatsaronis and Morosuk, 2018; Aktemur *et al.,* 2021). The experimental freezer effectively manages fresh blood plasma quality, reducing energy costs and making it economically feasible in industrialized countries. Motorized, temperature-controlled freezers are beneficial in low-income and emerging nations for heat-sensitive biological tissues (Traclet *et al.*, 2015; Smith *et al.,* 2013; Arcot *et al.,* 2020).

Both evaporator types-maintained plasma content quality for 48 hours off-cycle, while blast evaporator quality decreased beyond 72 hours due to energy loss from opening the service door. The plasma freezer design, including copper tubes and blast evaporators, is efficient for storing frozen plasma in resource-limited areas and transporting heat-sensitive medicinal supplies, maintaining quality for 48 hours off-cycle.

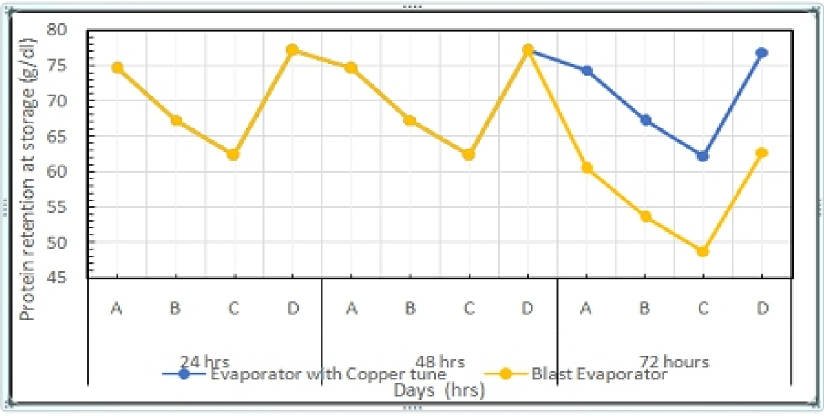

Figure 18: Comparison of Protein retention by blast and copper tube evaporators

4. **Conclusion**

The research developed a compact two-stage vapour compression refrigerator using a heat exchanger system and copper coil evaporator, powered by a 12 kg temperature-controlled storage capacity and a 5 kVA generator. Cattle blood plasma evaluated system performance, achieving 89.6% efficiency and 3.18 COP beyond storage hours. Deep-freezing system preserves plasma quality for 72 hours without recharge. The work compares two energy-efficient, portable, and fast-performing systems for frozen plasma solidification, including a copper tube evaporator that outperforms traditional refrigerators for long-term storage and rapid freezing. The blast evaporator model effectively freezes products to low temperatures, saving energy and stabilizing plasma proteins, extending shelf life, and enhancing heat-sensitive medicine management. Both techniques ensured uniform and effective freezing of plasma proteins when hanging on hangers, enhancing heat-sensitive drug handling. The device is recommended for efficient healthcare delivery in remote developing nations due to its energy-saving features and lower energy consumption compared to traditional freezers. The study suggests a compact system combining a copper tube and blast evaporator for addressing variations in freezing and defrosting times.

Acknowledgements

This research is fully sponsored by the Nigerian government through TETUND's Institution Based Research (IBR) with grant number TETF/DR&D/CE/UNI/EKITI/IBR/2021/VOL.II. The Vice Chancellor, Professor O.V. Adeoluwa, and the Centre for Research and Development (CERAD), Bamidele Olumilua University of Education, Science and Technology, Ikere-Ekiti (BOUESTI), are greatly appreciated for providing a conducive studying environment, promoting staff research development, and, most importantly, the success of this noble work.

Nomenclatures

Symbol	Description	Unit
A_{cci}	Surface area of the cooling chamber insulator	mm
ib	Inner breadth of the cooling chamber	mm
ih	Inner height of the cooling chamber	mm
wh	Inner width of the cooling chamber	mm
U	Overall heat transfer coefficient	W/m^2K
$\dot{H}_f$	Heat flow rate at freezing	kJ/s
A	Surface area of the evaporator	m^2
t	Time for frozen	hr
$\dot{H}_{ew}$	Heat flow rate in the evaporator's wall	kJ/s
H_f	Amount of heat flow at freezing	kJ
ΔT_o	Temperature change from ambient to freezing	K
M_p	Mass of blood plasma at ambient temperature	kg
C_p	Specific heat of frozen plasma below freezing	kJ/kgK
H_b	Product heat load before freezing	kJ/kg

ΔT_i	Temperature change inside evaporator	K
L_p	Latent heat of blood plasma	kJ/kg
M_i	Mass of plasma inside cooling chamber	kg
H_{inf}	Infiltration heat load	kJ/kg
C_a	Specific heat of air	J/kg-°C
$T_o - T_i$	Temperature change from ambient to cooling	K
$\mathbf{M}_{pk}$	Mass of packed product	kg
$\mathbf{C}_{pk}$	Package material specific heat	J/kg-°C
H_{pk}	Package material heat load	kJ/kg
H_r	Refrigeration load	kJ/kg
H_l	Heat rejected at PSS (LTC)	kJ/kg
H	Heat rejected at SSS (HTC)	kJ/kg
$\dot{m}_L$	Mass flow rate at PSS	kg/s
$\dot{m}_H$	Mass flow rate at SSS	kg/s
$(h_b - h_c)$	Heat addition at cascade condenser	kJ/kg
$(h_f - h_g)$	Heat rejected at SSS condenser	kJ/kg
$h_a - h_d$	Heat absorbed at PSS evaporator	kJ/kg
$h_e - h_h$	Heat absorbed at SSS evaporator	kJ/kg
$h_b - h_a$	Heat rejected at PSS compressor	kJ/kg
$h_f - h_e$	Heat rejected at SSS compressor	kJ/kg
C_e	Refrigerating effect	Jk/kg
Cce,h	Cascade refrigerating effect at heat exchanger	kJ/kg
$\dot{m}$	Mass flow rate	Kg/s
H_{ce}	Heat addition at cooling effect	kJ/kg
$\dot{m}_l$	Mass flow rate at LTC	Kg/s
P_r	Pressure ratio	
P_{rl}	Pressure ratio at PSS compressor	MPa
P_{dl}	Discharge pressure at PSS compressor	MPa
P_{sl}	Suction pressure at PSS compressor	MPa
P_r	Pressure ratio at SSS compressor	
P_d	Discharge pressure at SSS compressor	MPa
P_s	Suction pressure at SSS compressor	MPa
W_{comp}	Compressor work	kJ/kg
$W_{comp,l}$	Work done by compressor at PSS	kJ/kg
$W_{comp,h}$	Work done by compressor at PSS	kJ/kg
P_{comp}	Compressor power	W
$\mathbf{P}_{CL}$	Power consumed by PSS circuit	kW
$\mathbf{W}_{CL}$	Compressor work for PSS circuit	kJ/kg
$\mathbf{H}_r$	Heat rejected by condenser	kJ/kg
$\mathbf{P}_{CH}$	Power consumed by SSS circuit	kW
$\mathbf{H}_{rl}$	Heat rejected at PSS circuit	kJ/kg
$\mathbf{H}_{comp,h}$	Heat rejected at SSS circuit	kJ/kg
COP_c	Cascade condenser coefficient of performance	
COP_l	Coefficient of performance at PSS	
COP	Coefficient of performance at SSS	
COP_{ideal}	Reversed Cycle COP	
$COP_{ideal,l}$	Reversed Cycle COP for ideal at PSS	
$COP_{ideal,h}$	Reversed Cycle COP for ideal at SSS	
COP_{cas}	Cascade coefficient of performance	
n_L	System efficiency at PSS	%
$t_{e,l}$	Evaporator temperature at PSS	K
$t_{e,h}$	Evaporator temperature at SSS	K
$t_{c,l}$	Condenser temperature at PSS	K
$t_{e,h}$	Evaporator temperature at SSS	K
$t_{c,h}$	Condenser temperature at SSS	K
$COP_{a,h}$	Actual coefficient of performance at SSS	
W_{lc}	Compressor work at PSS	kJ/kg
W_{hc}	Compressor work at SSS	kJ/kg
I_{cas}	System Isentropic efficiency	%
RE_{cas}	System's relative effectiveness	%
W_{rev}	Reversed compressor work	kW
W_a	Actual compressor work	kW

References

Abdulghafor, I.A., Ali, S.A., Kadhim, S.A., AlMrayattee, H.M. andHammoodi, K.A. (2024). Exergy analysis of a solar heating system in indoor spaces. International Journal of Heat and Technology, 42(5), 1551-1558. https://doi.org/10.18280/ijht.420508

Adkins, J.N., Varnum, S.M., Auberry, K.J., Moore, R.J., Angell, N.H., Smith, R.D., Springer, D.L. and Pounds, J.G. (2022). Toward a human blood serum proteome: analysis by multidimensional separation coupled with mass spectrometry. Molecular and Cellular Proteomics, 1(12), 947 – 955.

Aktemur, C., Ozturk, I.T. and Cimsit, C. (2021). Comparative energy and exergy analysis of a subcritical cascade refrigeration system using low global warming potential refrigerants. Applied Thermal Engineering, 184, 16254. https://doi.org/10.1016/j.applthermaleng.2020.116254

Alhumaidan, H., Cheves, T., Holme, S. and Sweeney, J. (2010). Stability of coagulation factors in plasma prepared after a 24-hour room temperature hold. Transfusion, 50(9), 1934-1942.

Arcot, P. J., Kumar, K., Mukhopadhyay, T., and Subramanian, A. (2020). Potential challenges faced by blood bank services during Covid-19 pandemic and their mitigative measures: the Indian scenario. Transfusion Apheresis Science, 59(5), 102877.

Caramello, V., Camerini, O., Ricceri, F., Ottone, P., and Mascaro, G. (2019). Blood bank preparedness for mass casualty incidents and disasters: a pilot study in the piedmont region, Italy. Vox Sang, 114(1), 247 – 255.

Chakravarthy, M.A. and Deva-Kumar, M.L. (2012). Experimental investigation of an alternate refrigerant for R22 in window air conditioning system, International Journal of Scientific and Research Publication (IJSRP), 2(10), 2250-3153

Chen, Q., Zhou, L., Yan, G. and Yu, J. (2019). Theoretical investigation on the performance of a modified refrigeration cycle with R170/R290 for freezers application. International Journal of Refrigeration, 10(4), 282-290. https://doi.org/10.1016/j.ijrefrig.2019.05.037

Geyer, P.E., Kulak, N.A., Pichler, G., Holdt, L.M., Teupser, D. and Mann, M. (2016). Plasma proteome profiling to assess human health and disease. Cell System, 2(3), 185 - 195

Gratten, M., Battistutta, D. and Torzillo, P. (2018). Comparison of goat and horse blood as culture medium supplements for isolation and identification of haemophilus influenzae and Streptococcus pneumoniae from upper respiratory tract secretions. Journal of Clinical Microbiology, 8(32), 2871–2872.

Lemboye, K.T., Layemi, A.T., Oduntan, K., Akintunde, M.A. and Dahunsi, O.A. ()2015. Developing a two-stage cascade compressor arrangement for ice block production. Journal of Machinery Manufacturing and Automation, 4(2), 10 -16.

Leonardo, A.M., Guillermo, V.O. and Gaudy, P.B. (2018). Computer-aided simulation of the energetic efficiency of a two-stage cascade cooling system cycle. International Journal of Applied Engineering Research, 13(4), 11123-11125.

Malmstrom, E., Kilsgard, O., Haurl, S., Herwald, H., Malmstrom, L. and Malmstrom, J. (2016). Large-scale inference of protein tissue origin in gram-positive sepsis plasma using quantitative targeted proteomics; Nat Commun., 7(1), 10261-10273

Mondragon, L., Ochoa, G.V., and Botia, G.P. (2018). Computer-aided simulation of the energetic and exergetic efficiency of a two-stage cascade cooling cycle. International Journal of Applied Engineering Research,13(13), 11123-11128.

Mota-Babiloni, A., Mastani, J.M., Navarro-Esbrí, J., Mateu-Royo, C., Barrag´an- Cervera, A, and Amat-Albuixech, M. (2020). Ultralow-temperature refrigeration systems: Configurations and refrigerants to reduce the environmental impact. International Journal of Refrigeration, 111, 147–58.

Nagaraju, P., Kumar, C.K. and Manohar, M.V. (2015). Experimental study on performance parameters for refrigerants R22, R410a and R404a at various air outlet temperatures. International Journal of Engineering Research & Technology (IJERT), 4(2), 2278-0181

Oginni, O.T., Bolaji, B.O., Adetunla, A. and Kit, C.C. (202224). Advancement of a cascade refrigeration system for enhanced blood plasma preservation. International Journal of Heat and Technology, 42(6), 2039-2046, https://doi.org/10.18280/ijht.420621

Oginni, O.T., Bolaji, B.O., Oyelaran, O.A., Fadiji, E.A., Ige, A.M., and Oyerinde, Y.A. (2023).Thermodynamic performance analysis of cascade vapour refrigeration system using different refrigerant pairs : a review. Adeleke University Journal of Engineering and Technology (AUJET), 6(1)1, 132 – 145.

Pan, M., Zhao, H., Liang, D., Zhu, Y., Liang, Y. and Bao, G. (2020). A review of the cascade refrigeration system.Energies, 3(9), 234-246. https://doi.org/10.3390/en13092254

Prommas, R., Phiraphat, S. and Rattananadecho, P. (2019). Energy and exergy analyses of PV roof solar collector . International Journal of Heat and Technology,37(1), 303-312. https://doi.org/10.18280/ijht.370136

Rabbani, M.G., Karma, N., Patil, N., Wankhade, A. and Deshmukh, R. (2017). Cascade refrigeration system for blood storage.Dr. D. Y. Patil Institute of Technology, Pimpri,Pune / Savitribai Phule Pune University, India.

Rangare, A. and Mishra, P. (2019). A review on thermodynamic analysis of two stage cascade refrigeration system. International Journal for Science Research and Development, 7 (3), 2321 – 0613

Shukla, A., Dwivedi, M.K., Dubey, N. and Yadaw, A.K. (2018). Study of performance of a household refrigeration system with different refrigerants. International Journal of Engineering Research and Technology (IJERT), 7(6), 2278 - 0181

Smith, G.S., Walter, G.L., Walter, R.M., Haschek, W.M., Rousseaux, C.G. and Walling, M.A. (2013). Haschek and Rousseaux's Handbook of Toxicologic Pathology (Third edition), Clinical Pathology in NON-Clinical Toxicology Testing, Boston Academic Press, Chapter 18, 565 -594.

Traclet, J., Delaval, P., Terrioux. P. and Mornex, J.F. (2015). Augmentation therapy of alpha-1 antitrypsin deficiency associated emphysema. Revue des Maladies Respiratoires, 32(4), 435-46

Tsatsaronis, G. and Morosuk, T. (2018). Exergy analysis of cascade refrigeration system working with refrigerant pairs R41-R404A and Exergy analysis of cascade refrigeration system working with refrigerant pairs R41-R404A and R41-R161. International Journal of Heat and Temperature, 8(3), 132-14. https://doi.org/10.1088/1757-899X/377/1/012036

Upadhyay, S. and Pangtey, T. (2016). Quality analysis of blood component (PRBC and platelet concentrates): a study from a tertiary care teaching hospital of Kumaon region of Uttarakhand. Journal of Evolution Medical and Dental Sciences, 5(1), 1210-1212.

Ustaoglu, A., Kursuncu, B., Alptekin, M. and Gok, M.S. (2020). Performance optimization and parametric evaluation of the cascade vapor compression refrigeration cycle using Taguchi and ANOVA Methods. Applied Thermal Engineering, 180(4), 2134-2142. https://doi.org/10.1016/j.applthermaleng.2020.115816

Wang, H., Song, Y. and Cao, F. (2020). Experimental investigation on the pull-down performance of a -80°C ultra-low temperature freezer. International Journal of Refrigeration, 119(2), 1-10. https://doi.org/10.1016/j.ijrefrig.2020.04.030

World Health Organization. (2022). Global status report on blood safety and availability 2021, Geneva. World Health Organization, CC BY-NCSA 3.0 IGO.

Zhang, M., Sun, J. and Fricke, B. (2022). A study on computational fluid dynamics modeling of a refrigerated container for COVID-19 vaccine distribution with experimental validation. International Communications in Heat and Mass Transfer, 130(4), 105749.

Zhou, J., Le, S., Wang, Q. and Li, D. (2018). Optimization analyses on the performance of an auto-cascade absorption refrigeration system operating with mixed refrigerants. International Journal of Low- Carbon Technologies, 13(2), 212-217.